

A CFD MODEL FOR SIMULATING URBAN FLOW IN COMPLEX MORPHOLOGICAL STREET NETWORK

Saddok Houda¹, Nouredine Zemmouri², Abdelmalek Hasseine³, Rachid Athmani⁴, Rafik Belarbi⁵

¹University of Biskra, department of civil engineering, B.P. 145 R.P. 07000 Biskra, ALGERIA

²University of Biskra, department of architecture, B.P. 145 R.P. 07000 Biskra, ALGERIA

³Laboratory LARGHYDE University of Biskra, B.P. 145 R.P. 07000 Biskra, ALGERIA

⁴University of Biskra, department of mechanical engineering, B.P. 145 R.P. 07000 Biskra, ALGERIA

⁵Laboratory LEPTAB, University La Rochelle, France

Tel. +213661124163, Fax +213 33 74 51 74, e-mail:hasseine@yahoo.fr

Abstract: The present study considers an investigations of urban flow in complex morphological street network that is coincidentally similar to ancient Algeria city namely Ghardaïa. This study shows how one can apply a CFD model to simulate the air flow behavior in this urban area.

The computational fluid dynamics software, Fluent 6.3.26 is employed to determine velocity field traversing the streets. Information on the layouts of buildings in the selected area is contained in Google earth.

The AC3D 6.5.28, with its programming facility, has been used to extract the geometry of each building polygon under research. These are then cleaned by Materialise Magics and input into Gambit 2.4.6 the Fluent's mesh generation software to construct the simulations.

Finally, a steady-state simulation results are drawn from the velocity field profile.

Keywords: *CFD, Complex urban fabrics, Buildings, Urban Flow*

1. Introduction

There is a need to properly develop the application of Computational Fluid Dynamics (CFD) methods in support of air quality studies. CFD models are emerging as a promising technology for such assessments, in part due to the advancing power of computational hardware and software (Neophytou, 2005). CFD, simulations have the potential to yield more accurate solutions than other methodologies because it is a solution of the fundamental physics equations and includes the effects of detailed three-dimensional geometry and local environmental conditions. The results of CFD simulations can both be directly used to better understand specific case studies as well as be used to support the development of better-simplified algorithms that may be generally applied (Jal, 2003).

As the 3D solid model of the geometry was not available a captured Google Earth image of the fabric structure was used as a backdrop in the AC3D software, supplied as a utility to Fluent code software. The outlines of the buildings were then traced to create polygons, which were then extruded to produce the individual buildings.

The urban configuration being complex Gambit has been used to develop a specific un-structured meshing grid which takes into account the geometry of the buildings and the surroundings. Special attention was paid to the precise modeling and high grid resolution of the whole built environment

In this work we propose an approach – to model cities as obstacles characterized by an overall city form, building area density and street configuration, morphological characteristics that affect the structure and the intensity of wind entering, leaving, and flowing around and above cities. Studies of the impact of urban morphology on urban airflow are rare, although, ironically, this approach to understanding urban design was promoted by Vitruvius in the first century BC (Vitruvius, 1960). Skote et al. (2005) qualitatively investigated the flow pattern in round compact cities with one or two larger main streets and reinitiated by Hang et al.(2009) for two simple city forms such as a round

city form and a rectangular form each with a single or two intersecting main streets that dominate the otherwise compact city form.

Then the potential of CFD for prediction of wind speeds around a complicated urban environment and a complex fabric structures is investigated in this work.

The city of Ghardaïa, in the M'zab valley, may be taken as the case study with its dense fabric which demonstrates the ideas of building cool, shaded, airy structures in a hot dry climate.

This specific built environment with its complex and organic geometry will help to demonstrate the ability of CFD techniques to tackle the most complicated situations.

2. Mathematical model

2.1 Physical model

The commercial CFD code Fluent 6.3.26 (Fluent Ansys Inc., 2006) was used in this research. The 3D steady RANS equations are solved in combination with the realizable $k-\epsilon$ turbulence model. The realizable $k-\epsilon$ turbulence model is chosen because of its general good performance for wind flow around buildings (Franke et al., 2004). Pressure-velocity coupling is taken care of by the SIMPLE algorithm, pressure interpolation is standard and second order discretisation schemes are used for both the convection terms and the viscous terms of the governing equations.

All the objects that will be included in the simulation must be prepared in a step-by-step procedure starting with the capture of the area of investigation using Google Earth 4.2 Professional (Google Earth, 2007). The image is then imported in the AC3D software where the outlines of the buildings were traced and then extruded to produce the individual buildings (AC3D, 2009). The dimensions and the geometry of the objects are scaled to fit the real size of the configuration.



Fig.1 Ghardaia Complex Urban Morphology

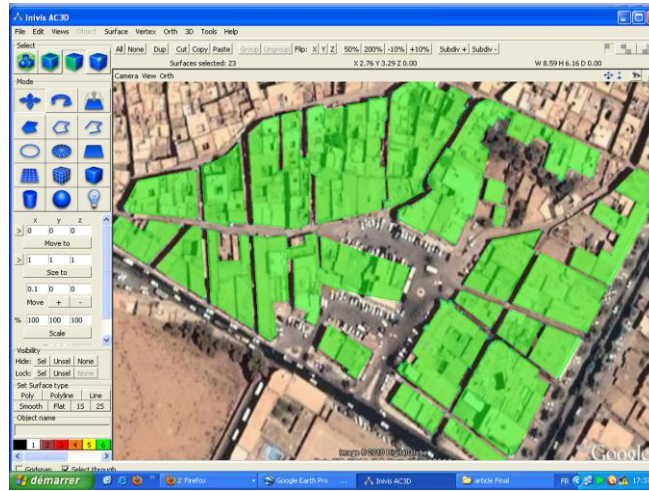


Fig.2 Tracing the Complex Urban Morphology Using AC3D

It is well known that the CAD files created or generated by CAD packages do not necessarily guarantee that the facets are consistent with each other in respect of inward- and outward-looking direction or define closed volumes. Fluent requires that facets should have a direction sense in order that it can know on which side is the fluid and on which the solid; and of course facets which share an edge should be in agreement on the matter. In most cases there is a need to fix and repair the overlapping surfaces in order to simulate complicated configurations. In the present case Magics 12.0 software (Materialise Magics, 2007) has been used to correct the file containing the urban geometry of the case study as shown in figures 3 and 4.



Fig.3 Defective 3D Urban Configuration Tracing Result Using AC3D

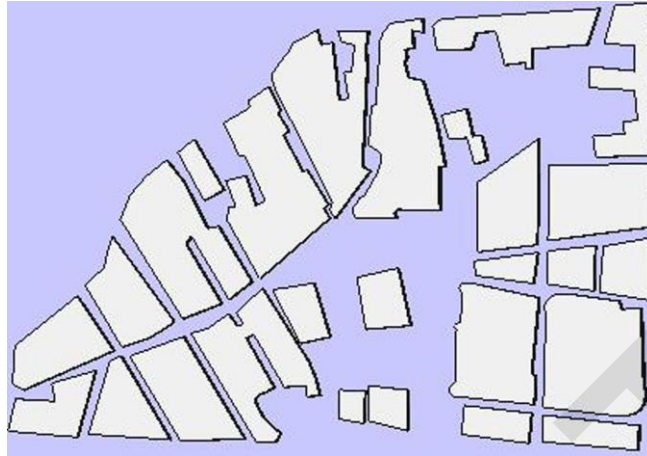


Fig.4 Repaired 3D Urban Configuration Tracing Result Using Magics

2.2 Numerical simulation

The governing equations of incompressible turbulent wind flow around buildings are continuity and the Reynolds-averaged Navier–Stokes equations, expressed as follows:

$$\frac{\partial U_i}{\partial x_i} = 0 \tag{1}$$

$$\frac{\partial U_i U_j}{\partial x_i} = -\frac{\partial P}{\partial x_i} + B_i + \rho \sum_j \left[\nu_L \left(\frac{\partial U_i}{\partial x_j} + \frac{\partial U_j}{\partial x_i} \right) - \overline{u_i u_j} \right] \tag{2}$$

1) Turbulence model

The turbulent stresses appeared in equation (2), use the eddy-viscosity concept to determine the Reynolds stresses from

$$-\overline{\rho u_j u_i} = \mu_\tau \left[\frac{\partial U_i}{\partial x_j} + \frac{\partial U_j}{\partial x_i} \right] - \rho K \frac{2d_{ij}}{3} \tag{3}$$

Where

$$\mu_\tau = C \rho V_s L_s \tag{4}$$

And where C is an empirical constant, and V_s and L_s are turbulence velocity and length scales which characterize the LARGE-SCALE turbulent motion.

A reasonable value of the kinematic eddy viscosity ν_τ can be estimated by taking as $C = 0.01$ and V_s as a typical mean-flow velocity and the length scale L_s as ~10% of the flow width

$$v_t = \frac{\mu_t}{\rho} \tag{5}$$

The standard high-Re form of the $k-\varepsilon$ model employs the following turbulence transport equations:

$$\rho \frac{\partial}{\partial x_i} \left[U_i K - \frac{v_t}{Pr_K} \frac{\partial K}{\partial x_i} \right] = \rho (P_K + \Gamma_b - \varepsilon) \tag{6}$$

$$\rho \frac{\partial}{\partial x_i} \left[U_i \dot{\rho} - \frac{v_t}{Pr_{\dot{\rho}}} \frac{\partial \dot{\rho}}{\partial x_i} \right] = \rho \frac{\varepsilon}{K} (C_{1e} P_K + C_{3e} \Gamma_b - C_{2e} \varepsilon) \tag{7}$$

The kinematic turbulent (or eddy) viscosity is given by:

$$v_t = C_\mu C_d \frac{K^2}{\varepsilon} \tag{8}$$

$$C_\mu = 0.5478 \quad C_d = 0.1643 \quad Pr_K \quad Pr_{\dot{\rho}}$$

The model constants are: Γ_b ; $\Gamma_b = 1.0$; $\frac{Pr_{\dot{\rho}}}{K} = 1.314$; $C_{1e} = 1.44$, $C_{2e} = 1.92$ and $C_{3e} = 1.0$.

The buoyancy production Γ_b is < 0 for stably-stratified layers, so that Γ_b is reduced and turbulence damped. For unstably-stratified layers, Γ_b is positive and turbulence is augmented.

The constant C_{3e} has been found to depend on the flow situation. It should be close to zero for stably-stratified flow, and close to 1.0 for unstably-stratified flows.

The default value of C_{3e} is 1.0.

3. Geometry and Solution Domain

Due to the complex geometry of the urban configuration and the large difference between the smallest and the largest length scales in the domain, generating a computational grid with good quality is not straightforward. In order to predict the flow field around a building with acceptable accuracy, the most important thing is to correctly reproduce the characteristics of separating flows near the roof and the walls. Therefore, a fine grid arrangement is required to resolve the flows near the corners. To handle the complex shaped domain of the case study the pre-processor Geometry and Mesh Building Intelligent Toolkit (GAMBIT) (Ansys Gambit, 2004) was used and results in unstructured grids of tetrahedral cells. The total number of cells is 913487-551593-174698-129211 for very fine, fine, medium and coarse meshings respectively. An overall view of the grids from is shown in figure 5 and a more detailed view is given in figure 6 for only one case.



Fig.5 Triangular Paved Mesh on Flow-volume Bottom Face of the Urban Configuration

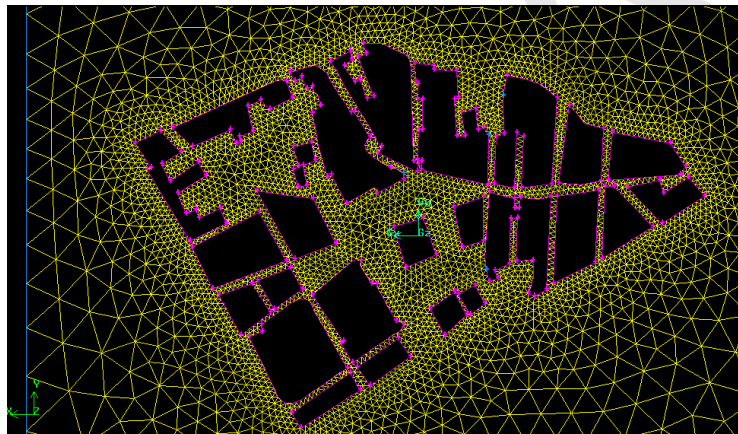


Fig.6 Characteristics of the Tetrahedral Elements Mesh for the Urban Configuration

To allow full control over the grid quality and resolution, the grid is constructed using the control mesh quality size functions to control mesh sizes in the regions adjacent to buildings geometry surfaces.

The size of the domain has been taken as a multiple of the characteristic height of the tallest building which is in this case 18 meters, as recommended by Hall (Hall, 1996) who suggests that the distance between any edge of the domain and the buildings must be at least five times of the characteristic height of the building.

The domain covers the entire area of 350m x 250m, including all the buildings and surrounding areas. The height of 50m from the ground in the vertical direction of the calculation domain provides about 30 m of open space above the tallest building.

4. Boundary conditions

An inflow condition was applied at the leftmost (upwind) side ($y-z$ plane) of the domain as given in Figure 7. An inlet wind speed of 25 m/s has been chosen as representing the average wind conditions in the region. In addition the orientation of the urban configuration has been selected according to the prevailing wind direction. Given that the computational domain is large enough, the boundary conditions for lateral and upper surfaces do not have significant influences on the calculated results around the target building (Mochida et al., 2002; Shirasawa et al., 2003; Yoshie et al., 2005).

A pressure outlet condition was applied at the rightmost (downwind) side ($y-z$ plane) of the domain. The remaining faces of the flow volume are taken as symmetry type expect for the base which has been specified as wall. The values of $k-\varepsilon$ were taken as (Robitu et al., 2006).

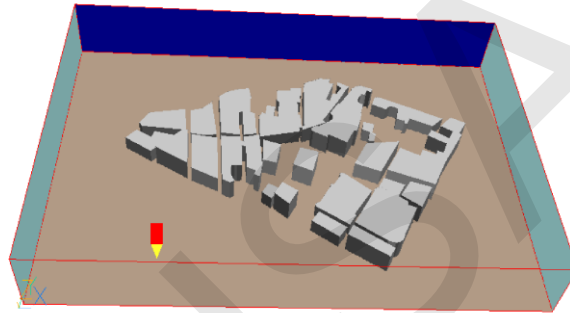


Fig.7 Setup of the 3D urban configuration for simulation

5. Solution of the equations

In Fluent 6.3.26 the pressure-velocity coupling in the incompressible flow is resolved through the SIMPLE algorithm of Patankar and Spalding (Patankar, 1972). The convective and diffusive equations are chosen according to the second order upwind discretization scheme employing a staggered grid. The first-order upwind scheme is not appropriate for all transported quantities, since the spatial gradients of the quantities tend to become diffusive due to a large numerical viscosity. COST also does not recommend the use of first-order methods like the upwind scheme except in initial iterations (Franke et al., 2004).

Calculation needs to be finished after sufficient convergence of the solution. For this purpose, it is important to confirm that the solution does not change by monitoring the variables on specified points or by overlapping the contours among calculation results at different calculation steps. In addition the scaled residuals have been dropped 4 orders of magnitude as suggested by COST (Franke, 2006). A stricter convergence criteria given by relaxation coefficients has been used to resolve the complexity of the case study geometry for the 4 different meshing to achieve the solution of the problem after 78-114-148-189 iterations respectively.

6. Results and discussion

The test of accuracy involved running the same simulation at different resolutions. This involved changing the spacing of the node points in GAMBIT for the creation of the mesh.

The smaller the spacing between node points, the greater the resolution, which means greater accuracy of the model.

Ideally one would want the highest resolution possible, but with a higher resolution it takes more processing power to compute the simulation.

Running a simulation at a low resolution may take seconds while at a higher resolution can take hours for the same number of iterations.

To find a good balance between speed and accuracy, this test was run at various resolutions.

More refined grids have been tested and it has been shown that the results remain unchanged.

The comparison between the flux results obtained at outlet area for the last two finer meshes are small and have approximately the same magnitudes 22690 W.

Images were generated to show various views of the velocity fields. The horizontal distribution of airflow at the height of 5 m in the sample area, whose size is 87500 meters square, is shown in Figure 8. At this scale, the shape and arrangement of individual buildings affect the formation of the field of wind.

It is seen from Figures 8 and 9 that the velocity of air flux varies drastically with urban density. In the present case the urban configuration acts as a wind shield reducing the air velocity inside the urban fabric, whereas the maximum velocities are observed at the boundaries of the lot. In large open spaces among buildings, although the wind direction is complicated, the wind speed is relatively low. In addition it is clear that dense and organic forms appear to create a better sheltered outdoor environment.

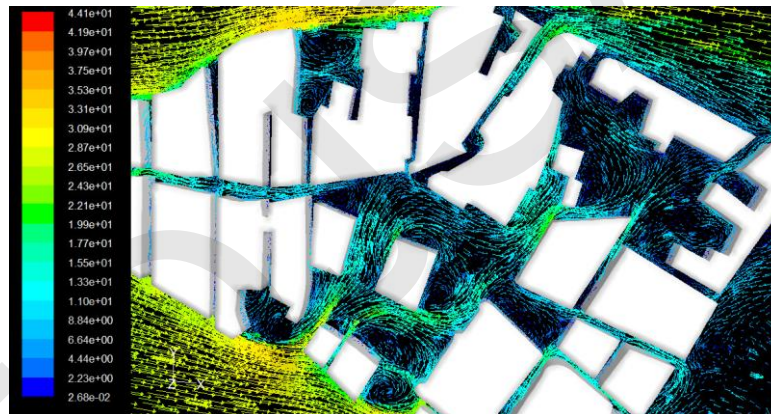


Fig.8 3D view of the horizontal distribution of airflow at the height of 5 m in the sample area

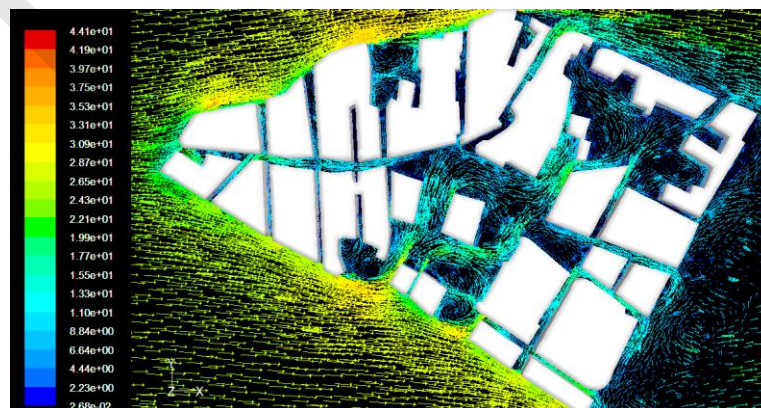


Fig.9 Scaled 3D view of the horizontal distribution of airflow at the height of 5 m in the sample area

Conclusions

Considerable effort has been made in recent years to improve the scientific understanding of air flow phenomena. CFD has been used as a modeling technique requiring long computational times and expensive hardware/software resources. However, recent computer hardware developments have contributed to the spread of CFD modeling, since the speed and memory capacities of PCs are now sufficient for relatively small applications.

However, a large number of research studies have focused on regular new geometric urban configurations overlooking the effects of vernacular old and complex urban fabrics which could be of interest to develop appropriate urban geometries under specific climate conditions.

A numerical study of velocity field in a densely vernacular urban fabric has been undertaken and discussed here. It was found that the velocity distribution can considerably change with the building shape and urban configuration. By using computational fluid dynamics (CFD) useful information can be drawn and used by urban developers, architectural designers and environmental planners to promote natural ventilation, a good measure for reducing energy use in buildings and providing better outdoor air quality. It has been also demonstrated the ability of combining different tools from picture capture, image correction to CFD simulation to assess a natural phenomena.

It should be kept in mind that the main objective of this research is to improve the understanding of the behavior of a system, rather than obtaining results readily comparable with regulatory standards.

References

- AC3D 6.5.28 copyright © 2009 Invis Ltd.
 Fluent 6.3.26, (2006). Ansys Inc.
 Franke, J., Hirsch, C., Jensen, A., Krüs, M., W., Schatzmann, M., Westbury, P., S., Miles, S., D., Wisse, J. A., Wright, N., G. (2004) Recommendations on the use of CFD in wind engineering. In: van Beeck, J. P. A. J. (Ed.), COST Action C14, Impact of Wind and Storm on City Life Built Environment. *Proceedings of the International Conference on Urban Wind Engineering and Building Aerodynamics*, 5–7.
 Franke, J. (2006). Recommendations of the COST action C14 on the use of CFD in predicting pedestrian wind environment. *The Fourth International Symposium on Computational Wind Engineering, Yokohama, Japan, July*.
 Google Earth Version 4.2 2007.
 Gambit 2.4.6, (2004). Ansys Inc.
 Hang, J., Sandberg, M., Yuguo Li. (2009). Effect of urban morphology on wind condition in idealized city models / *Atmospheric Environment* 43 870 869–878.
 Hall R., C. Evaluation of modeling uncertainty – CFD modeling of near-field atmospheric dispersion. (1996). Project *EMU final report*. WS Atkins Consultants Ltd, UK.
 Jal. E (2003). Applying CFD to environmental flows. *Report of Connell Wagner Pty Ltd, Australia*, Materialise Magics Version 12.0.1.2 2007.
 Mochida, A., Tominaga, Y., S. Murakami, S., Yoshie, R., Ishihara, T., Ooka, R., (2002). Comparison of various $k - \epsilon$ models and DSM applied to flow around a high-rise building. *Report on AIJ cooperative project for CFD prediction of wind environment. Wind Struct.* 5 (2–4), 227–244.
 Neophytou, M., Britter, R. (2005). Modeling the wind flow in complex urban topographies: A computational-fluid-dynamics simulation of the central London area. *5th GRACM International Congress on Computational Mechanics Limassol*,
 Patankar, S., Spalding, D. (1972). A calculation procedure for heat, mass and momentum transfer in three-dimensional parabolic flows. *International Journal of heat and mass transfer*, Vol. 15.
 Robitu, M., Musy, M., Inard, C., Dominique Groleau. (2006). Modeling the influence of vegetation and water pond on urban microclimate / *Solar Energy* 80 435–447
 Skote, M., Sandberg, M. U. Westerberg, (2005). Numerical and experimental studies of wind environment in an urban morphology. *Atmospheric Environment* 39, 6147–6158.

- Shirasawa.T, Tominaga.T, Yoshie.T, Mochida.R, Yoshino.A, Kataoka.H, H. Nozu, T. (1960).
Development of CFD method for predicting wind environment around a high-rise building part 2: the cross comparison of CFD results using various $k - \epsilon$ models for the flow field around a building model with 4:4:1 shape. *AIJ J. Technol. Des.* 18, 169–174.
- Vitruvius, M.P. *The Ten Books of Architecture*. Dover, New York.
- (2003). Development of CFD method for predicting wind environment around a high-rise building part 2: the cross comparison of CFD results using various $k - \epsilon$ models for the flow field around a building model with 4:4:1 shape. *AIJ J. Technol. Des.* 18, 169–174.
- Yoshie.R, Mochida.A, Tominaga. Y, Kataoka. Y, Harimoto.K, Nozu.T, Shirasawa.T.(2004).
Cooperative project for CFD prediction of pedestrian wind environment in Architectural Institute of Japan. *J. Wind Eng. Ind. Aerodyn.* 95, 1551–1578.